

AD \_\_\_\_\_

Award Number: DAMD17-94-J-4287

TITLE: Analysis of the Regulation of Expression of Transforming  
Growth Factor-Beta in Human Breast Cancer Cells

PRINCIPAL INVESTIGATOR: Bradley Arrick, M.D., Ph.D.

CONTRACTING ORGANIZATION: Dartmouth College  
Hanover, New Hampshire 03755-3580

REPORT DATE: October 1999

TYPE OF REPORT: Final

PREPARED FOR: U.S. Army Medical Research and Materiel Command  
Fort Detrick, Maryland 21702-5012

DISTRIBUTION STATEMENT: Approved for public release  
distribution unlimited

The views, opinions and/or findings contained in this report are those  
of the author(s) and should not be construed as an official Department  
of the Army position, policy or decision unless so designated by other  
documentation.

20001020 040

DTIC QUALITY INSPECTED 4

**REPORT DOCUMENTATION PAGE**Form Approved  
OMB No. 074-0188

Public reporting burden for this collection of information is estimated to average 1 hour per response, including the time for reviewing instructions, searching existing data sources, gathering and maintaining the data needed, and completing and reviewing this collection of information. Send comments regarding this burden estimate or any other aspect of this collection of information, including suggestions for reducing this burden to Washington Headquarters Services, Directorate for Information Operations and Reports, 1215 Jefferson Davis Highway, Suite 1204, Arlington, VA 22202-4302, and to the Office of Management and Budget, Paperwork Reduction Project (0704-0188), Washington, DC 20503

<b>1. AGENCY USE ONLY (Leave blank)</b>		<b>2. REPORT DATE</b> October 1999	<b>3. REPORT TYPE AND DATES COVERED</b> Final (01 Oct 94 - 30 Aug 99)	
<b>4. TITLE AND SUBTITLE</b> Analysis of the Regulation of Expression of Transforming Growth Factor-Beta in Human Breast Cancer Cells			<b>5. FUNDING NUMBERS</b> DAMD17-94-J-4287	
<b>6. AUTHOR(S)</b> Bradley Arrick, M.D., Ph.D.				
<b>7. PERFORMING ORGANIZATION NAME(S) AND ADDRESS(ES)</b> Dartmouth College Hanover, New Hampshire 03755 - 3580  e-mail: bradley.arrick@dartmouth.edu			<b>8. PERFORMING ORGANIZATION REPORT NUMBER</b>	
<b>9. SPONSORING / MONITORING AGENCY NAME(S) AND ADDRESS(ES)</b> U.S. Army Medical Research and Materiel Command Fort Detrick, Maryland 21702-5012			<b>10. SPONSORING / MONITORING AGENCY REPORT NUMBER</b>	
<b>11. SUPPLEMENTARY NOTES</b>				
<b>12a. DISTRIBUTION / AVAILABILITY STATEMENT</b> Approved for public release distribution unlimited			<b>12b. DISTRIBUTION CODE</b>	
<b>13. ABSTRACT (Maximum 200 Words)</b>  This combined final report for the research and career development grants relates to three objectives. Work on the first objective first focused on an analysis of the importance of TGF- $\beta$ expression as a determinant of clinical outcome. No such correlation was evident. Subsequent experiments examined the importance of a functionally intact TGF- $\beta$ signaling pathway with regards to tumor necrosis factor (TNF)-mediated cytotoxicity of MCF-7 cells, and documented that derepression of Bcl-2 expression as a consequence of loss of TGF- $\beta$ responsiveness likely underlies the acquired resistance to TNF. The second objective centered around an in vivo model of tumorigenicity and metastatic potential of breast cancer cells altered with regard to their production of and responsiveness to TGF- $\beta$ . Distinct paracrine and autocrine roles for TGF- $\beta$ were highlighted, with local invasiveness determined to be largely a paracrine effect of TGF- $\beta$ . The most rapid tumor growth was evident with the cells that remained responsive to TGF- $\beta$ however. The third objective was to identify the molecular determinants of promoter usage for TGF- $\beta$ 3 in breast cancer cell lines. Hypomethylation at a small grouping of CpGs in breast cancer cells was identified as a molecular correlate of downstream promoter activation.				
<b>14. SUBJECT TERMS</b> Breast Cancer			<b>15. NUMBER OF PAGES</b> 26	
			<b>16. PRICE CODE</b>	
<b>17. SECURITY CLASSIFICATION OF REPORT</b> Unclassified	<b>18. SECURITY CLASSIFICATION OF THIS PAGE</b> Unclassified	<b>19. SECURITY CLASSIFICATION OF ABSTRACT</b> Unclassified	<b>20. LIMITATION OF ABSTRACT</b> Unlimited	

## FOREWORD

Opinions, interpretations, conclusions and recommendations are those of the author and are not necessarily endorsed by the U.S. Army.

\_\_\_\_ Where copyrighted material is quoted, permission has been obtained to use such material.

\_\_\_\_ Where material from documents designated for limited distribution is quoted, permission has been obtained to use the material.

\_\_\_\_ Citations of commercial organizations and trade names in this report do not constitute an official Department of Army endorsement or approval of the products or services of these organizations.

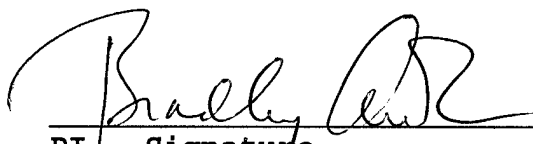
\_\_\_\_ In conducting research using animals, the investigator(s) adhered to the "Guide for the Care and Use of Laboratory Animals," prepared by the Committee on Care and use of Laboratory Animals of the Institute of Laboratory Resources, national Research Council (NIH Publication No. 86-23, Revised 1985).

☒ For the protection of human subjects, the investigator(s) adhered to policies of applicable Federal Law 45 CFR 46.

☒ In conducting research utilizing recombinant DNA technology, the investigator(s) adhered to current guidelines promulgated by the National Institutes of Health.

☒ In the conduct of research utilizing recombinant DNA, the investigator(s) adhered to the NIH Guidelines for Research Involving Recombinant DNA Molecules.

\_\_\_\_ In the conduct of research involving hazardous organisms, the investigator(s) adhered to the CDC-NIH Guide for Biosafety in Microbiological and Biomedical Laboratories.

  
PI - Signature 12/28/99  
Date

## **FINAL REPORT**

**Grant Numbers DAMD17-J-4287 & DAMD17-J-4130**

**PI:** Bradley A. Arrick, M.D., Ph.D.

**Institution:** Dartmouth College

**Reporting Period:** 10/1/94-9/30/99

### **Titles:**

Analysis of the Regulation of Expression of Transforming Growth Factor-beta in Human Breast Cancer Cells (#4287)

&

Studies on Human Breast Cancer and Transforming Growth Factor-beta --  
Application for a Career Development Award (#4130)

### **Table of Contents**

Front Cover	i
SF 298 Form	ii
Foreword	iii
Table of Contents	1
Introduction	2
Body of Report	2-15
Key Research Accomplishments	16
Reportable Outcomes	16
Conclusions	17
References Cited	18
Appendices	

## **FINAL REPORT**

### **Grant Numbers DAMD17-J-4287 & DAMD17-J-4130**

**PI:** Bradley A. Arrick, M.D., Ph.D.

**Institution:** Dartmouth College

**Reporting Period:** 10/1/94-9/30/99

#### **Titles:**

Analysis of the Regulation of Expression of Transforming Growth Factor-beta in Human Breast Cancer Cells (#4287)

&

Studies on Human Breast Cancer and Transforming Growth Factor-beta -- Application for a Career Development Award (#4130)

## **Introduction**

This final report includes the combined accomplishments of two grants (#4287 and #4130). The combining of the two grants was made on the recommendation of a USAMRMC Breast Cancer Research Project Site Visit, conducted on the campus of Dartmouth College on December 4, 1997. The site visit panel's final recommendations included modification of the Statement of Work (SOW) to reflect some of the changes in scientific focus that had occurred during the course of this research, merging of the Statements of Work for the two grants into one (since one of the grants was a career development award funding partial effort on some of the same research), and consolidation of all subsequent reports for the two grants into one. The combined grant was approved for a 5<sup>th</sup> year at a no-cost extension. This report is therefore a combined final report, based on the revised SOW.

## **Body of Report**

### **Objective #1**

Summary of prior annual reports. In prior annual reports, we provided data which suggested that earlier indications that high levels of tumor cell expression of TGF- $\beta$  correlated with a poor clinical outcome did not apply to an independent set of breast cancer patients all of whom had node-positive disease at presentation. We had also reported that few if any breast cancers (<20%) have gene amplification of the TGF- $\beta$ 1 locus. At that point in the research, with the approval of the site visit team, attention turned to an analysis of the importance of a functional TGF- $\beta$  signalling pathway with regard to susceptibility to tumor necrosis factor (TNF)-mediated cytotoxicity of MCF-7 cells. In last year's report, data were presented that demonstrated that abrogation of TGF- $\beta$  responsiveness, achieved by stable expression of a dominant negative truncated TGF- $\beta$  type II receptor, resulted in the acquisition of relative resistance to TNF.

Examination of upstream mediators of TNF action, and some of the known cellular mechanisms for TNF resistance, highlighted the fact that the TGF- $\beta$ -resistant MCF-7 cells expressed much higher levels of Bcl-2, which has been known to protect cells from TNF-mediated cytotoxicity.

#### Results from final year

One of our objectives for the final year of research on this objective was to characterize the apoptosis-related phenomenon that accompanies TNF-toxicity. Multiple attempts to detect and quantitate activation of caspases, such as via cleavage of the enzyme PARP yielded no evidence of such an event subsequent to TNF exposure. This was not entirely unexpected, given that MCF-7 cells have been reported to lack caspase 3, a key enzyme responsible for proteolytic cleavage events (Tang et al., 1998). Similarly, many investigators have reported that DNA laddering is not typically seen in MCF-7 cells following apoptosis. We had thusfar characterized TNF-cytotoxicity by the MTS assay following a 5 day exposure. Since the MTS assay simply measures cell number, in light of the above findings, to distinguish actual cytotoxicity from simple proliferation inhibition we examined cells following exposure to TNF for viability, as measured by the ability to exclude trypan blue. Cells were treated with 1000 U/ml of TNF for 5 days, at which time cell counts with trypan blue were performed. At that time point, viability of the MCF-7/EZ control cell clones was  $28.7 \pm 4.7\%$ , whereas the viability if the TGF- $\beta$  nonresponsive MCF-7/TREZ cell clones was  $60.0 \pm 7.6\%$  (p value = 0.0002). This served to confirm that actual cytotoxicity, and not simply growth arrest, was occurring.

Further experiments were performed to rule out the involvement of either NF- $\kappa$ B or p53 as determinants of the TNF resistance of the MCF-7/TREZ TGF- $\beta$ -nonresponsive cells. By western analysis, we have determined that the MCF-7/EZ and MCF-7/TREZ clones did not differ significantly with regard to p53 expression level (not shown). In the prior year, we reported that induction of nuclear NF- $\kappa$ B DNA binding activity, as measured by the gel shift assay, in response to TNF treatment did not differ comparing MCF-7/EZ and MCF-7/TREZ clones. With reports that in some instances NF- $\kappa$ B transcriptional activity does not always directly correlate with DNA binding activity (Newton et al., 1999), we sought to confirm our conclusion that alterations in NF- $\kappa$ B did not underly the TNF resistance of the MCF-7/TREZ cells by transfection of cells with a NF- $\kappa$ B-responsive luciferase reporter construct. In these experiments cells were plated in 10 cm dishes and transfected with 9  $\mu$ g of the NF- $\kappa$ B responsive p-55lgkLuc plasmid (Fujita et al, 1993) by lipofectAMINE (Life Technologies). The following day each dish of cells was trypsinized and the cells divided equally among the wells of a 6-well plate. Cells were treated in duplicate with 0, 100, or 300 U/ml TNF- $\alpha$  at 37°C for 20 h. To prepare lysates, cells were washed 3 times with cold PBS, suspended in 200  $\mu$ l of lysis buffer (1% Triton-X100, 25 mM glycylglycine, 15 mM MgSO<sub>4</sub>, 4 mM EGTA, 1 mM DTT), then centrifuged at 14,000  $\times$  g for 5 min at 4°C to pellet insoluble material. The supernatant was assayed for luciferase activity in triplicate in a luminometer.

Luciferase activity of each sample was normalized to protein content of the lysate, which was assessed by BCA protein assay (Pierce). Data are represented in Figure 1.

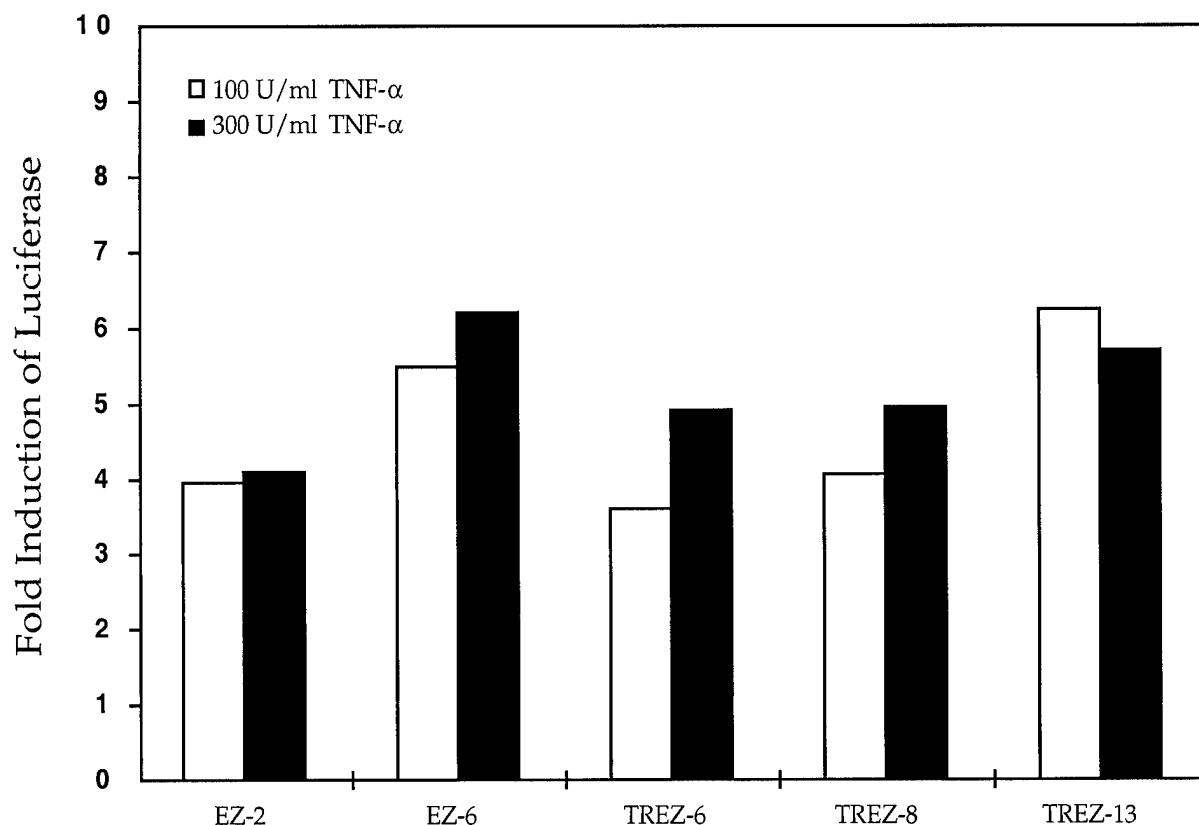


**Figure. 1. Autocrine TGF- $\beta$  signaling does not alter TNF- $\alpha$  induced levels of NF- $\kappa$ B activity.** Cells were transfected with the NF- $\kappa$ B responsive luciferase reporter plasmid p-55Ig $\kappa$ Luc. The next day, the cells were treated with 0, 100, or 300 U/ml of TNF- $\alpha$  for 20 h, then assayed for luciferase activity. Each bar represents the average of duplicate lysates that were analyzed for luciferase activity in triplicate, and are expressed as fold-induction compared to the cells in the absence of TNF. Standard deviations of the triplicate samples averaged less than 4% of the mean. TNF-induced NF- $\kappa$ B activation in MCF-7/EZ clones was not significantly different from that in MCF-7/TREZ clones ( $p > 0.6$ ).

Our results suggested that abrogation of TGF- $\beta$  responsiveness in MCF-7 cells resulted in an upregulation of Bcl-2, i.e. that TGF- $\beta$  serves to repress the expression of Bcl-2, and that this was the only evident etiology for the differences in TNF susceptibility. In cell systems other than breast epithelial cells, malignant or normal, TGF- $\beta$  has been reported to either upregulate or downregulate expression of Bcl-2 (Prehn et al, 1994; Motyl et al,

1998; Hague et al, 1998). We therefore thought it important to further investigate the effect of TGF- $\beta$  on Bcl-2 expression in MCF-7 cells. Our approach was to restore TGF- $\beta$  signaling to a subline of MCF-7 cells that had lost its responsiveness to TGF- $\beta$ . It has been documented that through prolonged passage, sublines of MCF-7 cells have arisen that are no longer responsive to TGF- $\beta$  (Ko et al, 1998). We have obtained such a variant of MCF-7 cells, i.e. cells that have spontaneously lost TGF- $\beta$  responsiveness. These cells are not growth inhibited by TGF- $\beta$ , are resistant to TNF- $\alpha$ -mediated cell death, and express a level of Bcl-2 comparable to the MCF-7/TREZ cells (data not shown). Activation of the TGF- $\beta$  signal transduction cascade in these cells was achieved by transfection of a novel expression construct for a chimeric protein in which the cytoplasmic kinase domains of T $\beta$ RI and T $\beta$ RII are tethered to each other, thereby bypassing any receptor defect (Feng and Derynck, 1996). In three separate transient transfections of this construct, in which transfection efficiencies of 30-40% were assessed by parallel transfections of an expression plasmid for green fluorescent protein, Bcl-2 protein levels were reduced to 50% of transfected controls on average and this reduction is statistically significant ( $p = 0.027$ ). Figure 2 includes western analysis data from two such experiments.



**Fig. 2. Restoration of TGF- $\beta$  signaling results in a decrease in Bcl-2 expression.** A TGF- $\beta$  nonresponsive subline of MCF-7 cells were transfected with the plasmid pXF1042 or the empty vector control, EZ. The pXF1042 construct expresses a chimeric protein containing the cytoplasmic kinase-containing domains of T $\beta$ R-I and T $\beta$ R-II, which has been shown to activate TGF- $\beta$  signaling in the absence of ligand. Parallel transfections of an expression plasmid for green fluorescent protein, pEGFP-N3 (Clontech), yielded estimated transfection efficiencies of 30-40%. Protein lysates were harvested 3 days after the transfection and Bcl-2 expression (arrow) was analyzed by western blot, loading 30  $\mu$ g of total protein per lane.



As expected for transient transfection experiments in which only a fraction of the total cell population have activated the TGF- $\beta$  signaling cascade through expression of the chimeric receptor construct, the observed level of Bcl-2 protein was not as low as that observed in the TGF- $\beta$  responsive MCF-7/EZ stable transfectants.

Further proof that the derepression of Bcl-2 expression resulting from abrogation of the TGF- $\beta$  pathway was the underlying reason that these cells had acquired relative resistance to TNF was sought by incubating MCF-7/TREZ cells with an antisense oligonucleotide to Bcl-2. If we could specifically diminish Bcl-2 levels in these cells and thereby restore their TNF susceptibility, we could exclude the possibility that other, as yet undetermined alterations in the MCF-7/TREZ cells mediated their TNF resistance. Bcl-2 antisense oligonucleotides capable of downregulating Bcl-2 levels in other cell systems have been reported (Ziegler et al., 1997). We, however, have thusfar been unable to similarly downregulate Bcl-2 levels in our cells, using the exact oligos and transfection methods of the published reports.

The data relating to objective #1 will soon be submitted for publication.

### **Objective #2**

This overall goal of this Objective is to evaluate the *in vivo* tumorigenic capacity of breast cancer cells with altered expression levels of TGF- $\beta$  and/or diminished responsiveness to TGF- $\beta$ . In last year's report, we provided data from an experiment in which nude mice were injected with subclones of the MDA-MB231 human breast cancer cell line which differed in terms of TGF- $\beta$  production or responsiveness. We reported that the tumors derived from C2C2 cells (cells which overexpress active TGF- $\beta$ ) were larger and had necrotic centers, whereas the p-CEN-derived control cell tumors were smaller, pearly white in color throughout, and without necrotic centers. Abrogation of the TGF- $\beta$  autocrine loop in the C2S2 cells (by the double transfection with TREZ) diminished the growth potential of these cells, but central necrosis persisted.

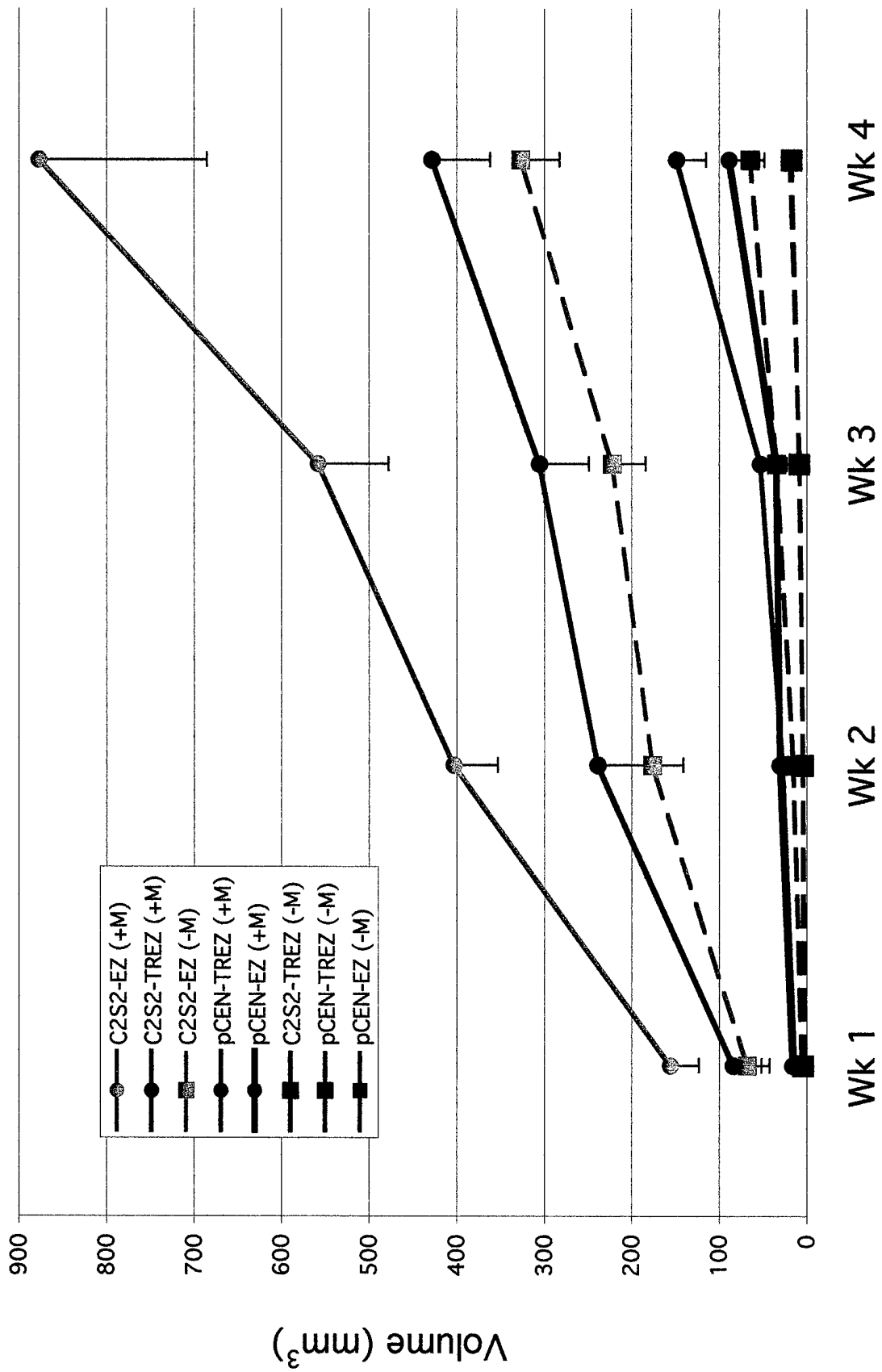
Additional *in vivo* experiments were performed in the 5<sup>th</sup> year of this work. Figure 3 includes data from weekly tumor measurements from all experiments combined. As suggested by our initial experiment, the TGF- $\beta$ -overexpressing C2S2 cells had the highest growth rate and produced the largest tumors throughout the experiment. Comparison of the C2S2-EZ clone to the C2S2-TREZ clone, which lacks a functional autocrine loop, indicates that both autocrine and paracrine effects of TGF- $\beta$  are necessary for the enhanced primary tumor growth demonstrated by the C2S2-EZ cells.

*Actual figure is on the next page*

**Figure 3. Weekly volumes of primary tumors** Athymic nude mice at 6-7 weeks of age were injected subcutaneously with  $3 \times 10^6$  cells with or without matrigel. Each week the primary tumors were measured in two dimensions with calipers and tumor volumes were calculated as  $\text{Volume} = L \times S^2 \times 0.52$  where L is the longer diameter and S is the shorter diameter. Each curve represents the average volumes of 12 mice injected with the same cell clone and the error bars depict standard error of the mean (SEM).

The rapid growth of the C2S2-EZ cells *in vivo* contrasted with our observations during routine cell culture that they proliferated more slowly *in vitro*. In experiments to measure anchorage-dependent growth rates of the clones, each clone was counted and plated identically in three 96-well plates. These replica plates were analyzed by MTS cell proliferation assay (one plate per day) for a three day time course. The MTS assay is a colorimetric assay that provides a measure of the relative number of metabolically active cells. The linearity of this assay with cell number was verified by analyzing a plate containing a dilution series of cell suspensions of known densities. The data generated from the three day time course was graphed and the slopes of the growth curves compared to evaluate relative growth rates. We determined that both of the pCEN-derived clones grow faster than the C2S2 clones. The pCEN-TREZ clone exhibited a growth rate that was only slightly faster than that of the pCEN-EZ control (110% of control). The C2S2-EZ clone grew the slowest (65% of control) while C2S2-TREZ displayed an intermediate growth rate (80% of control). The fact that each TREZ clone grows faster than its EZ counterpart is consistent with loss of the autocrine signaling loop, thereby releasing the cells from TGF- $\beta$ 's growth inhibition. Indeed, it is not surprising that the C2S2-EZ clone, secreting large amounts of active TGF- $\beta$  while maintaining a functional receptor complex, displays the slowest growth rate of the group.

In addition to comparing the adherent growth rates of the clones, we examined the clones with regards to their propensity to grow in a semi-solid suspension. An assay commonly used to measure anchorage independent growth is the soft agar colony-forming assay, in which a single-cell suspension of each clone is plated in a semi-solid mixture of growth media and 0.35% agar. This suspension is plated over a solidified layer of 0.7% agar and cooled briefly to allow the 0.35% layer to solidify. The cells remain suspended and therefore must grow without contact with the tissue culture plastic. The cells were incubated at 37°C for two weeks and then the colonies were counted. We recorded colonies in three size ranges, 4-10 cells, 11-20 cells and greater than 20 cells. The data are represented in figure 4 on page 9.



These data indicate that the two pCEN clones are more capable than the C2S2 clones at forming anchorage independent colonies. The pCEN clones have more than twice the total number of colonies than the C2S2 clones and the distribution is shifted such that 30-40% of pCEN colonies are greater than 10 cells in size, while only 15% of C2S2 colonies grow to exceed the 10 cell size.

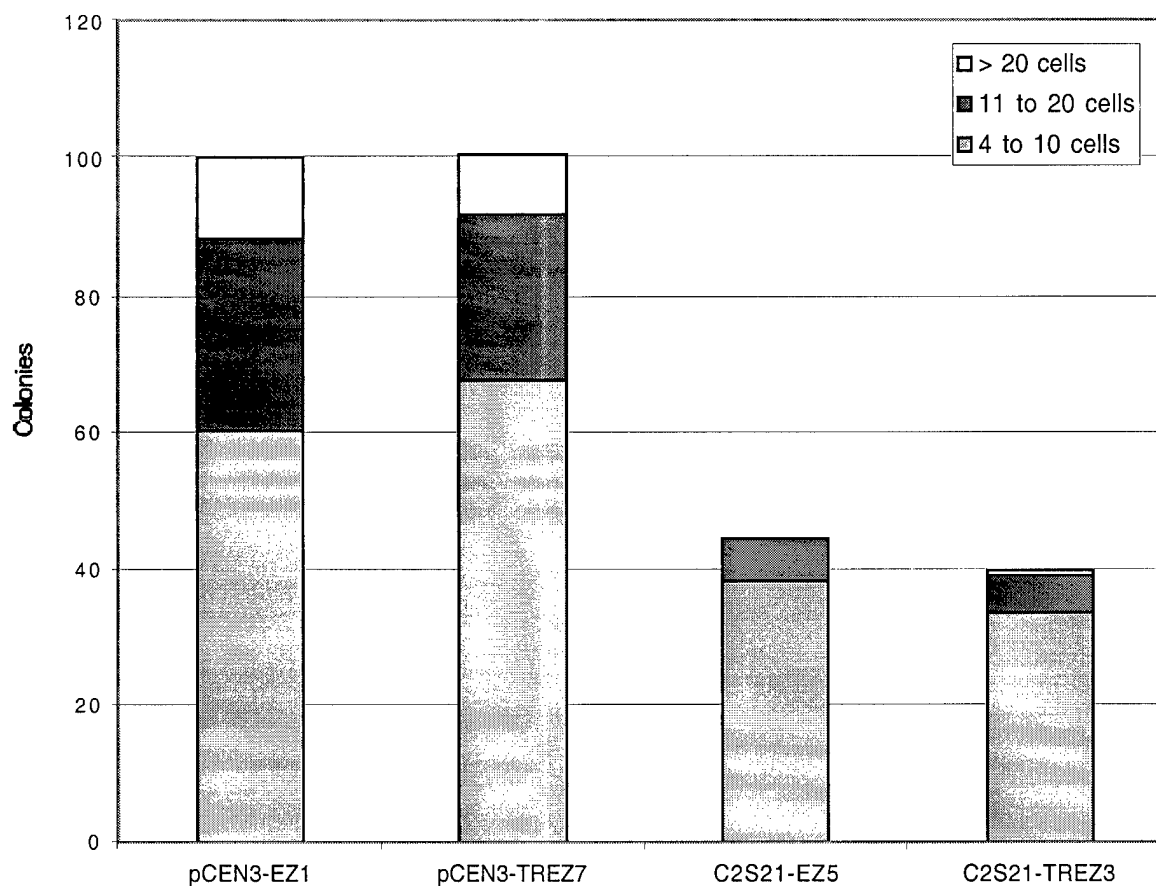


**Figure 4. pCEN clones are more adept than C2S2 clones at *in vitro* anchorage independent growth.** The four MDA-231 double transfectants were evaluated for their propensity for anchorage independent growth in a soft agar colony forming assay. Cells were counted, suspended in serum-containing media containing 0.35% agar, and this suspension was overlaid on a solidified 0.7% agar bed. Following a brief cooling period to solidify the 0.35% layer, the cells were incubated at 37°C, 5% CO<sub>2</sub> for 2 weeks and colonies of at least 4 cells were scored. The total colony number counted was corrected for the potential colony forming units counted at the start of the two week growth period.

Thus, there was no appreciable difference between pCEN-EZ and pCEN-TREZ or C2S2-EZ and C2S2-TREZ in this anchorage independent growth assay.

In order to evaluate the effect of alterations in TGF- $\beta$  production and/or responsiveness on the metastatic capability of a tumor, we measured the frequency and amount of metastatic spread of the four MDA-231 double transfectants in the xenograft mouse model. Two methods were employed to detect metastatic spread of the tumor cells. The first is a sensitive PCR based strategy used to detect tumor cell DNA in a sample of gDNA harvested from a target organ and the second is the more classical approach of microscopic examination of tissue sections from the target organs. The lung and liver are common targets of metastatic disease in breast cancer and as such, were chosen for our study of the formation of spontaneous metastases in the xenograft model. Upon sacrifice of the mice, two samples of each tissue were harvested. One sample was processed for the preparation of gDNA and the second was fixed in formalin and paraffin-embedded for the preparation of tissue sections.

We started our analysis of metastatic spread using the PCR based strategy with the thought that employing the sensitivity of PCR may facilitate the detection of micrometastases that may be missed by traditional histological review of tissue sections. PCR primers were designed for the detection of plasmid sequence in the vectors used to generate the stable transfectants. Specifically, one primer is directed against the IRES sequence and one primer is directed against the zeocin resistance gene. These sequences are present in both the EZ and TREZ constructs and yield the same product from both constructs. Additionally, all four of the stable clones are double transfectants so each clone contains either EZ or TREZ integrated into their gDNA. Normal mouse gDNA (mice not injected with any tumor cells) was used as a negative control to confirm that these primers did not produce nonspecific PCR products from mouse gDNA. Following PCR amplification of the gDNA samples the products were subjected to southern analysis to verify the specificity of the PCR product and perhaps further enhance the sensitivity over that of an ethidium bromide stained gel. The probe for southern analyses was made using a fragment from the EZ vector that overlapped the sequence amplified by the PCR primers. In order to quantitate the amount of tumor DNA detected in a given sample (i.e. the metastatic burden), we ran a dilution series of tumor cell gDNA diluted in normal mouse gDNA with each PCR/southern as an internal standard curve. The southern blots were scanned and the samples that were positive for metastasis were quantitated by comparison to the standards. An example of one scanned southern blot with standard curve is shown in figure 5. The metastatic spread of each tumor was also evaluated by histology using H+E stained sections of tissue. These analyses correlated well with the results obtained by PCR/southern analysis. It should be noted however, that a couple of samples thought to be negative based on review of the H+E stained lung sections were positive for metastasis by PCR,

demonstrating the sensitivity of the PCR/southern methodology. No metastases were detected in the liver of any mice.

## STANDARDS

## LUNG DNA FROM INDIVIDUAL MICE



**Figure 5. Southern analysis of PCR products from gDNA harvested from the lungs of mice injected with C2S2-TREZ.** Southern analysis to detect metastatic spread of tumor cells from the primary tumor to the lung. Following a 5 week period of growth of the xenograft tumor, the mice were sacrificed and lung tissue collected for harvesting gDNA. 100ng of gDNA was used as template in PCR reactions using primers directed at vector sequence present only in the injected tumor cells. To facilitate quantitating the metastatic burden detected in the positive lung samples, an internal standard curve (shown to left) was generated using a dilution series of tumor cell gDNA diluted in normal mouse gDNA (3%, 0.3%, 0.03%, and 0.003% from left to right). The percent burden of each positive sample was calculated by linear interpolation using the two standards with band intensities that bracketed that of the sample. The values calculated for these six positive C2S2-TREZ samples are the following: 0.086%, 0.0195%, 0.149%, 0.00013%, 0.00056%, 0.0176% from left to right.

Table 1 provides a summary of the PCR/southern results indicating the frequency of metastasis for each clone and the metastatic burden found in the lung. These data indicate that the C2S2 clones displayed a higher incidence of metastatic spread than the pCEN clones. The total incidence for pCEN-EZ was 8 of 24 while C2S2-EZ tumors metastasized in 15 of 20 cases. The difference in these incidence rates is statistically significant ( $p=0.005$ ). Similarly, the total incidence of metastasis in pCEN-TREZ was 3 of 23, while that of C2S2-TREZ was 14 of 24 and this difference is also statistically significant ( $p=0.0008$ ). There were no significant differences in incidence of metastases when comparing a given clone with and without matrigel, as were there no significant differences between EZ and TREZ clones. These data suggest that tumor cells expressing high levels of TGF- $\beta$  are more likely to form a metastatic lesion.

In addition to determining incidence of metastasis, we calculated a percent metastatic burden for each positive sample. Average metastatic burden for each clone is shown in Table 1 and these data suggest that C2S2 clones tend to result in higher metastatic burden, either through formation of a greater number of metastatic lesions, larger metastatic lesions or both. On average, the four pCEN clones resulted in a metastatic burden of 0.0065% and the four C2S2 clones were 20-fold higher with an average

metastatic burden of 0.145%. Note that a metastatic burden of 0.1% means that on average 0.1% of the gDNA harvested from the lungs of tumor-bearing mice was tumor-derived. For the purpose of statistical analysis, the data were transformed by multiplying each percent burden value by 1000, adding 1 and then taking log of this result. A graphical representation of these data are shown in figure 6. In terms of statistical significance, all C2S2-clones with the exception of C2S2-TREZ without matrigel ( $p=0.52$ ) had significantly higher metastatic burden when compared to its pCEN counterpart (all  $p$  values  $< 0.05$ ). As was determined for incidence of metastasis, these data indicate that tumor cells expressing high levels of TGF- $\beta$  have an advantage in forming and maintaining metastatic lesions in the lung.

Clone Designation (+/- matrigel)	Lung Metastases		
	Incidence	Burden (%)	Range
pCEN-EZ-	4/12	.002	0-.014
pCEN-EZ+	4/12	.002	0-.015
pCEN-TREZ-	4/12	.02	0-.15
pCEN-TREZ+	1/12	.002	0-.023
C2S2-EZ-	7/10	.35	0-3.0
C2S2-EZ+	8/10	.11	0-.51
C2S2-TREZ-	5/12	.01	0-.062
C2S2-TREZ+	9/12	.11	0-.724

**Table 1. C2S2 clones are more metastatic than pCEN clones as measured by frequency and metastatic burden.** Summary of results from PCR/Southern analysis measuring frequency and burden of metastases to the lung. The differences in incidence of metastasis between C2S2 and pCEN clones are statistically significant (pCEN-EZ vs C2S2-EZ,  $p=0.005$ ; pCEN-TREZ vs C2S2-TREZ,  $p=0.0008$ )

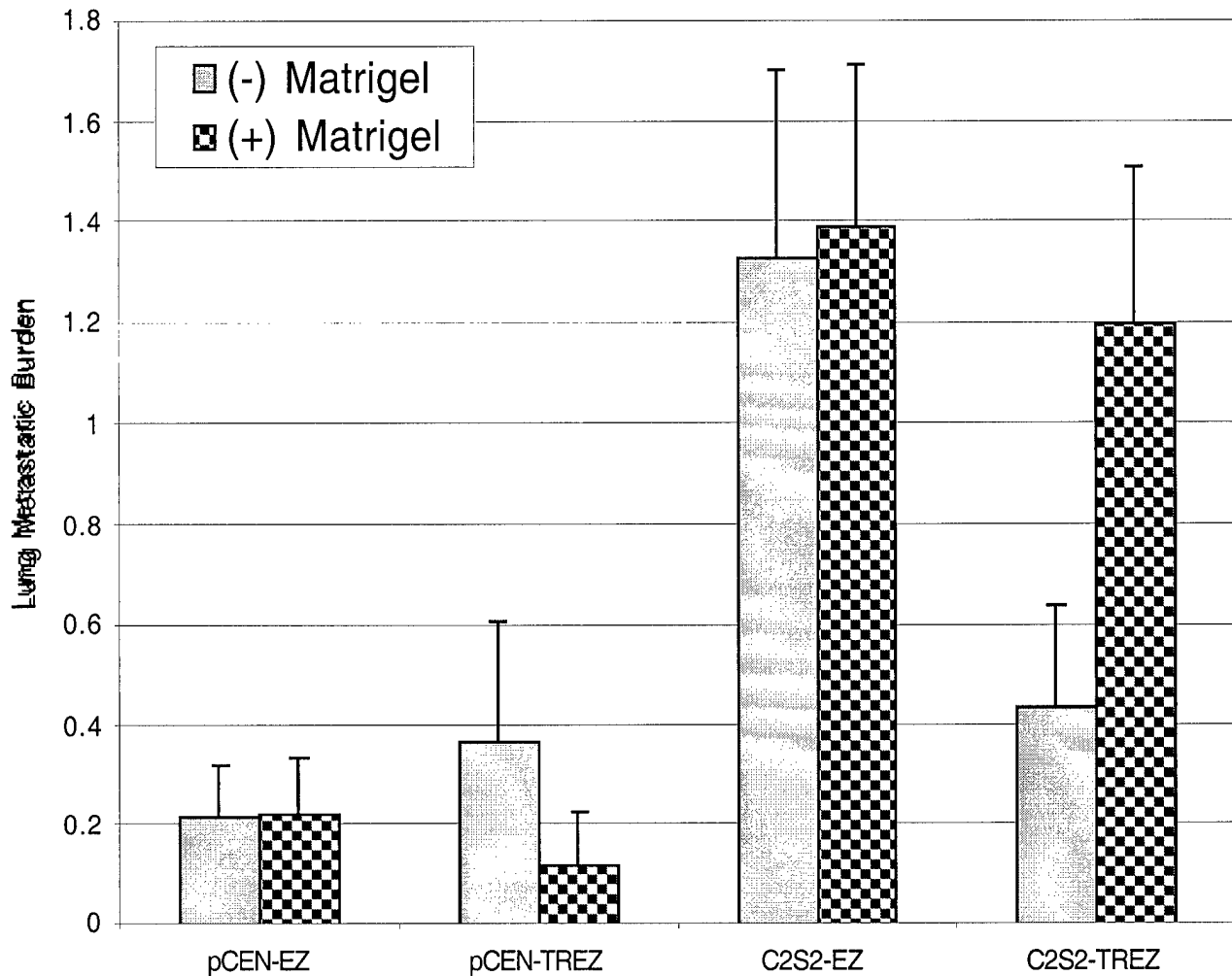


**Figure 6. Lung metastatic burden as determined by PCR followed by southern analysis.** A quantitative value for the metastatic tumor burden in the lung was determined by PCR of gDNA and southern analysis, as in figure 5. For the purpose of statistical analysis, these data were transformed by multiplying each percent burden value by 1000, adding 1 and then taking log of this result. The transformed data are plotted here, with error bars representing the SEM. With the exception of C2S2-TREZ injected without matrigel ( $p=0.52$ ), all of the C2S2 clones had a higher lung metastatic burden when compared to its pCEN counterpart and the differences are statistically significant. Specifically, C2S2-EZ (-) matrigel is greater than pCEN-EZ (-) matrigel ( $p=0.025$ ), C2S2-EZ (+) matrigel is greater than pCEN-EZ (+) matrigel ( $p=0.0056$ ), and C2S2-TREZ (+) matrigel is greater than pCEN-TREZ (+) matrigel ( $p=0.0029$ ).



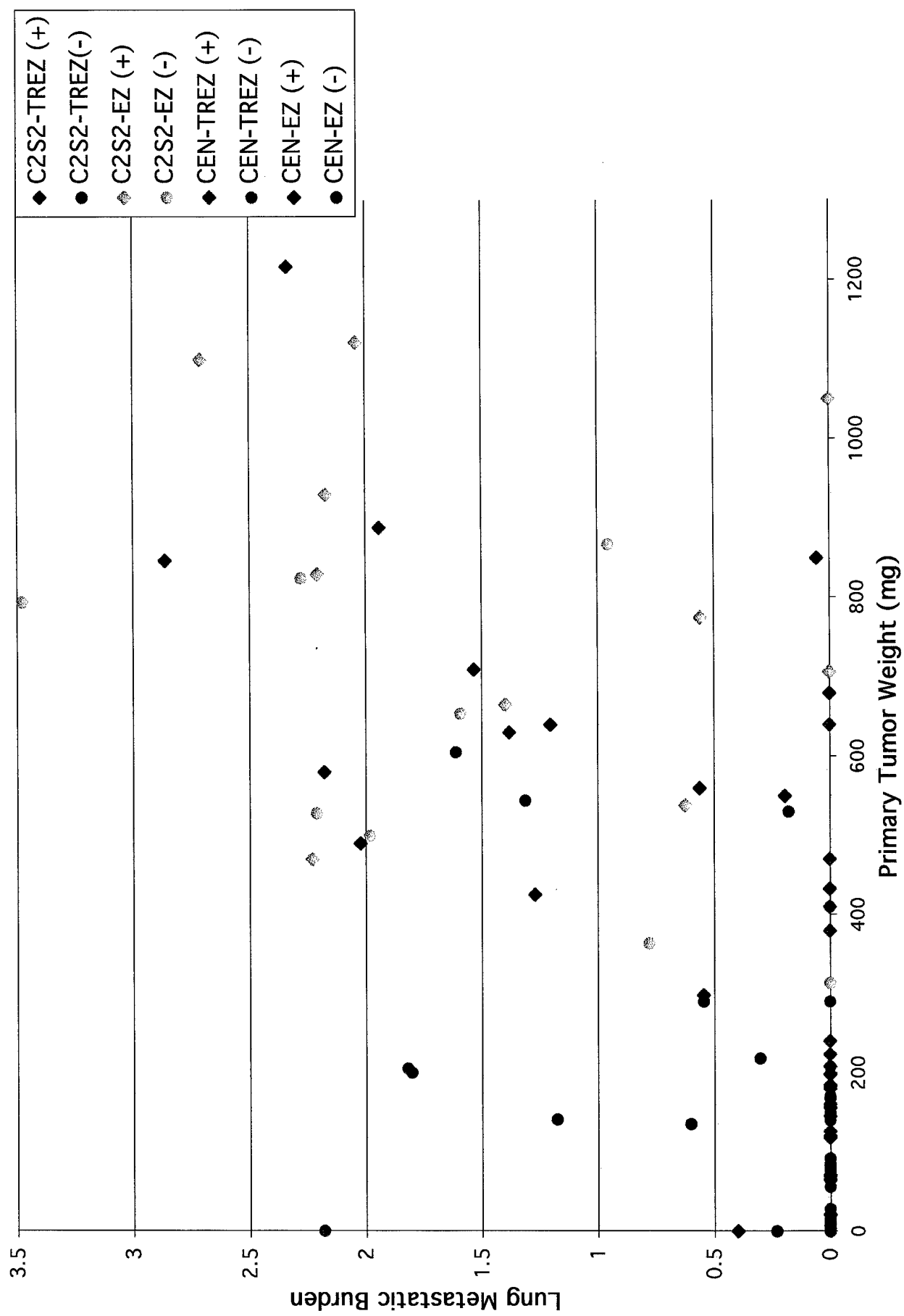
Finally, we analyzed the data from these *in vivo* experiments to determine if there was any relationship between the size of the primary tumor and the metastatic burden of the lung. Figure 7 is a graph of the lung metastatic burden of each mouse versus the final weight of its primary tumor. Each point on the graph represents one mouse. The plot shows that, as one might expect, there exists a general trend that larger primary tumors cause a higher metastatic burden to the lung. Therefore, we reevaluated our comparison of the metastatic capability of C2S2 clones as compared to pCEN clones in the context of the influence of tumor size on metastasis. Restricting the size of the primary tumors to a range of 250-800 mg to minimize the effect of primary tumor size, we again compared the lung metastatic burden of C2S2 clones versus pCEN clones. This size range was chosen because it contained a significant number of each tumor type. Statistical analysis indicates that within this size range there is no significant difference between the primary tumor sizes of C2S2 clones compared to pCEN clones, however the C2S2 clones produce a 3-fold higher lung metastatic burden and this difference is significant ( $p=0.015$ ).

*This figure is on the next page*

**Figure 7. Lung metastatic burden versus final weight of the primary tumor.** The lung metastatic burden of each mouse was plotted against the final weight of its primary tumor. Each point of the plot represents one mouse.

### **Objective #3**

This objective deals with an observation we have previously reported regarding the promoter usage for TGF- $\beta$ 3. Specifically, we have observed that a downstream promoter (P2) is activated in breast cancer cells, but not in any other cell line thus far examined (Arrick et al., 1994). The essence of the experiments under this objective were to understand the role of CpG methylation as a determinant of promoter usage. The results from this work have been published in this past year (a copy of that paper is included in the appendix in lieu of being detailed here).



## **Key Research Accomplishments**

- Expression of TGF- $\beta$ 1 in a group of node-positive breast cancer patients did not correlate with clinical outcome.
- Amplification of the TGF- $\beta$ 1 locus is not commonly observed in breast cancers.
- Loss of TGF- $\beta$  responsiveness can result in acquisition of relative resistance to TNF, perhaps due to derepression of Bcl-2 expression.
- In a nude mouse model, overexpression of TGF- $\beta$  augmented *in vivo* tumor growth, despite slower *in vitro* growth.
- Tumor-derived TGF- $\beta$ , via paracrine mechanisms, enhances the local invasiveness and metastatic capacity of MDA231 cells.
- The activation of a downstream alternative TGF- $\beta$ 3 promoter in breast cancer cells correlates with a notable demethylation at CpG sites in proximity to the transcription initiation site.

## **Reportable Outcomes**

### **Publications:**

1. Archey WB, Sweet MP, Alig GC, and Arrick BA. (1999) *Cancer Res.* 59:2292-2296.
2. Manuscript relating to objective #1 to be submitted
3. Manuscript relating to objective #2 to be submitted

### **Cell lines developed:**

1. Transfected clones of MCF-7 cells with abrogation of TGF- $\beta$  signalling (MCF-7/TREZ)
2. Transfected clones of MDA231 cells with increased TGF- $\beta$  expression and/or abrogation of TGF- $\beta$  signalling.

### **Degrees obtained:**

Stephen Tobin received a PhD degree in August 1999, in part due to research reflected in this report.

## **List of Personnel**

Bradley Arrick

Anne Cole

Karen Douville

Bruce Fuller (Student)

Stephen Tobin (Student)

Jennifer Myers (Student)

Meiling Lu (Student)

Graham Alig (Student)

Matt Sweet (Student)

## **Conclusions**

From the work encompassed in objective 1, we can conclude that within the subgroup of node-positive breast cancer patients, the level of expression of TGF- $\beta$ 1 as determined via immunohistochemistry did not predict clinical outcome. Furthermore, the TGF- $\beta$ 1 genetic locus is rarely amplified in breast cancers. An intact TGF- $\beta$  signalling loop may affect the responsiveness of breast cancer cells to apoptotic insults, such as TNF. Specifically, abrogation of TGF- $\beta$  responsiveness in MCF-7 cells resulted in an augmented expression level of Bcl-2 and an acquisition of a measure of TNF resistance.

Objective 2 utilized a panel of transfected cell clones from the MDA231 cell line which differed in the amount of TGF- $\beta$  produced by the cells, as well as in their innate responsiveness to TGF- $\beta$ . These cells were used in an *in vivo* nude mouse xenograft model to demonstrate that increased production of TGF- $\beta$  by the tumor in this system resulted in augmented tumor growth by both autocrine and paracrine mechanisms. In contrast, the tendency for local invasiveness, central necrosis, and distant metastasis was largely a paracrine effect.

Objective 3 uncovered a marked difference in CpG methylation pattern at the TGF- $\beta$ 3 locus comparing breast cancer cells and non breast cancer cells. This difference was consistent with the previously recognized breast cancer-specific utilization of a downstream promoter which generates a more translationally-competent transcript.

## References Cited

- Arrick, Bradley A., Richard L. Grendell, and Loree A. Griffin. 1994. Enhanced translational efficiency of a novel transforming growth factor- $\beta$ 3 mRNA in human breast cancer cells. *Molecular and Cellular Biology* 14:619-628.
- Feng X.H. and Derynck R. (1996) Ligand-independent activation of transforming growth factor (TGF)  $\beta$  signaling pathways by heteromeric cytoplasmic domains of TGF- $\beta$  receptors. *J. Biol. Chem.* 271:13123-13129.
- Fujita T., Nolan G.P., Liou H.-C., Scott M.L. and Baltimore D. (1993) The candidate proto-oncogene *bcl-3* encodes a transcriptional coactivator that activates through NF- $\kappa$ B p50 homodimers. *Genes Devel.* 7:1354-1363.
- Hague A., Bracey T.S., Hicks D.J., Reed J.C. and Paraskeva C. (1998) Decreased levels of p26-Bcl-2, but not p30 phosphorylated Bcl-2, precede TGF $\beta$ 1-induced apoptosis in colorectal adenoma cells. *Carcinogenesis* 19:1691-1695.
- Ko Y., Banerji S.S., Liu Y., Li W.H., Liang J.R., Soule H.D., Pauley R.J., Willson J.K.V., Zborowska E. and Brattain M.G. (1998) Expression of transforming growth factor- $\beta$  receptor type II and tumorigenicity in human breast adenocarcinoma MCF-7 cells. *J. Cell. Physiol.* 176:424-434.
- Motyl T., Grzelkowska K., Zimowska W., Skierski J., Wareski P., Ploszaj T. and Trzeciak L. (1998) Expression of *bcl-2* and *bax* in TGF- $\beta$ 1-induced apoptosis of L1210 leukemic cells. *Eur. J. Cell Biol.* 75:367-374.
- Newton, T. R., N. M. Patel, P. Bhat-Nakshatri, C. R. Stauss, R. J. Goulet, Jr., and H. Nakshatri. (1999) Negative regulation of transactivation function but not DNA binding of NF- $\kappa$ B and AP-1 by I $\kappa$ B $\beta$ 1 in breast cancer cells. *J. Biol. Chem.* 274:18827-18835.
- Prehn J.H., Bindokas V.P., Marcuccilli C.J., Krajewski S., Reed J.C. and Miller R.J. (1994) Regulation of neuronal Bcl2 protein expression and calcium homeostasis by transforming growth factor type beta confers wide-ranging protection on rat hippocampal neurons. *Proc. Natl. Acad. Sci. USA* 91:12599-12603.
- Tang, D. and V. J. Kidd. (1998) Cleavage of DFF-45/ICAD by multiple caspases is essential for its function during apoptosis. *J. Biol. Chem.* 273:28549-28552.
- Ziegler A., Luedke G.H., Fabbro D., Altmann K., Stahel R.A., and Zangemeister-Wittke U. (1997) Induction of apoptosis in small-cell lung cancer cells by an antisense oligonucleotide targeting the Bcl-2 coding sequence. *J. Natl. Cancer Inst.* 89:1027-1036.

# Methylation of CpGs as a Determinant of Transcriptional Activation at Alternative Promoters for Transforming Growth Factor- $\beta$ 3<sup>1</sup>

William B. Archey, Matthew P. Sweet, Graham C. Alig, and Bradley A. Arrick<sup>2</sup>

Departments of Physiology [W. B. A.] and Medicine [M. P. S., G. C. A., B. A. A.], Dartmouth Medical School, Hanover, New Hampshire 03755

## Abstract

The human transforming growth factor- $\beta$ 3 (*TGF- $\beta$ 3*) gene has a typical CpG island, the core of which is centered just upstream of its principle promoter. Activation of an alternative downstream promoter, leading to the production of a truncated mRNA lacking the portion of the 5' non-coding region responsible for translational inhibition of *TGF- $\beta$ 3* mRNA, is only evident in breast cancer cells. We compared the methylation status of genomic DNA isolated from a panel of breast (SKBR-3 and T47-D) and non-breast cancer (HT-1080, A673, and A375) cell lines by sequencing sodium metabisulfite-treated DNA. In all cell lines, the core of the *TGF- $\beta$ 3* CpG island was predominantly unmethylated, irrespective of promoter usage associated with that cell line. In contrast, we observed a marked difference in methylation at 19 CpG sites immediately flanking and downstream of the alternative promoter's transcription initiation site. Specifically, the non-breast cancer cell lines exhibited nearly complete methylation of these CpG sites, whereas in the breast cancer cell lines, these CpGs were predominantly unmethylated. Our data support the hypothesis that methylation of a limited number of CpGs at the periphery of an otherwise unmethylated CpG island underlies the transcriptional repression of the downstream promoter in non-breast cancer cells, thereby serving to regulate the use of alternative promoters for *TGF- $\beta$ 3*.

## Introduction

DNA methylation is becoming an increasingly appreciated epigenetic mechanism of transcriptional control. Methylation of such CpG-rich regions in the 5' flanking region of certain genes, termed CpG islands, is thought to inhibit transcription by directly impeding the binding of transcription factors to their *cis*-acting sites and/or by promoting the binding of methyl-DNA binding proteins, which restrict access of transcription factors to the DNA (1, 2). In normal adult tissue cells, CpG islands are generally unmethylated, whereas in some neoplastic cells, selected genes with CpG islands undergo *de novo* methylation. In a variety of human cancers, methylation of selected CpG islands has been correlated with repressed transcription of a number of different genes, including the estrogen receptor (3, 4), progesterone receptor (4), retinoblastoma protein (5), E-cadherin (6), *BRCA1* (7), and others.

The human *TGF- $\beta$ 3* gene has a typical CpG island, the core of which is centered just upstream of its principle promoter. The full-length mRNA of *TGF- $\beta$ 3* is expressed as a 3.5-kb transcript in many human cell types (8). Prior work in this laboratory has shown that this transcript includes a 1.1-kb 5' noncoding region that, largely because it includes multiple small open reading frames, inhibits translation of

*TGF- $\beta$ 3* (9, 10). One strategy for augmenting production of *TGF- $\beta$ 3* protein is the generation of a mRNA transcript that lacks the translational inhibitory sequences in the 5' noncoding region. This has been observed in breast cancer cells, where activation of an alternative downstream promoter results in the production of a 2.6-kb *TGF- $\beta$ 3* mRNA transcript lacking the most inhibitory portion of the 5' non-coding region (10). Thus, two promoters have been documented for *TGF- $\beta$ 3*: the initially characterized upstream promoter ( $P_1$ ), which directs transcription of the full-length translation-compromised 3.5-kb transcript, and a downstream promoter ( $P_2$ ), which yields the breast cancer-specific 2.6-kb transcript with enhanced translational capacity.

The work presented here deals with our investigation into whether specific patterns of CpG methylation at the *TGF- $\beta$ 3* gene locus correlate with promoter usage. Using a sodium metabisulfite treatment of genomic DNA to differentiate between methylated and unmethylated CpG dinucleotides (11), we observed a significant difference in the incidence of methylation at 19 CpG dinucleotides within and around the  $P_2$  region when comparing breast cancer cell lines to non-breast cancer cell lines. Our data suggest that the lack of DNA methylation in and around  $P_2$ , although limited to a relatively small number of CpGs at the periphery of the CpG island, allows for transcription of the 2.6-kb mRNA *TGF- $\beta$ 3* transcript in breast cancer cell lines. In contrast, hypermethylation of these CpG sites is associated with repression of transcription from  $P_2$  in non-breast cancer cell lines.

## Materials and Methods

**Cell Culture.** Cell lines were obtained from the American Type Culture Collection (Manassas, VA) and cultured in DMEM:Ham's F-12 medium, supplemented with 100 IU/ml of penicillin, 125  $\mu$ g/ml of streptomycin, 2 mM L-glutamine, and 10% fetal bovine serum. Cell cultures were maintained in a humidified incubator at 37°C under 5% CO<sub>2</sub>.

**RNA Isolation and Analysis.** Total cellular RNA from adherent cells grown on plastic was prepared by guanidinium thiocyanate-phenol extraction and analyzed by Northern blot with a <sup>32</sup>P-labeled 650-bp *Bgl*III fragment from the coding region of *TGF- $\beta$ 3* cDNA, as described previously (10).

**Bisulfite Modification of DNA.** Genomic DNA was isolated from adherent cells using the Puregene DNA isolation Kit (Gentra Systems, Minneapolis, MN), per the manufacturer's instructions. Prior to treatment with bisulfite, DNA was digested with either *Bgl*III (for the analyses shown in Figs. 2 and 3) or *Pst*I (for the analyses shown in Fig. 4). DNA digestions were extracted with buffer-saturated phenol and 24:1 chloroform:isoamyl, precipitated with EtOH, and resuspended in Tris-EDTA buffer.

A slight modification of the method of Raizis *et al.* (11) was used for the bisulfite treatment. In brief, fresh 2.5 M metabisulfite in water was mixed with freshly prepared 500 mM hydroquinone in a 2:1 ratio, and the pH was adjusted to 5.0 with 2 M NaOH. Before treatment with bisulfite, the digested DNA was denatured by incubation in 0.1 ml of 0.3 M NaOH for 15 min at 37°C. Bisulfite treatment was performed by adding 0.9 ml of the sodium bisulfite-hydroquinone solution to the denatured DNA sample. Reactions were then overlaid with mineral oil, wrapped in foil, and incubated at 55°C for 4 h. Following bisulfite treatment, DNA was desalted using the Wizard DNA Clean-Up System (Promega, Madison, WI) as described by the manufacturer's instructions. Desulphonation of sulfonated uracils was effected in 0.3 M NaOH. Finally, the DNA

Received 1/8/99; accepted 3/29/99.

The costs of publication of this article were defrayed in part by the payment of page charges. This article must therefore be hereby marked *advertisement* in accordance with 18 U.S.C. Section 1734 solely to indicate this fact.

<sup>1</sup> This work was supported by the United States Department of Defense Army Breast Cancer Program Grants DAMD17-94-J-4287 and DAMD17-94-J-4130. W. B. A. was supported in part by the Rosaline Borison Memorial Fund.

<sup>2</sup> To whom requests for reprints should be addressed, Phone: (603) 650-1550; Fax: (603) 650-1129; E-mail: Bradley.Arrick@dartmouth.edu.

<sup>3</sup> The abbreviations used are: *TGF- $\beta$ 3*, transforming growth factor- $\beta$ 3; UTR, untranslated region.

was precipitated in EtOH, washed with 70% EtOH, and resuspended in TE buffer.

**Genomic Sequencing of Bisulfite-treated DNA.** Selected regions of the TGF- $\beta$ 3 genomic locus were amplified from bisulfite-modified DNA by nested PCR. To amplify the regions upstream of P<sub>1</sub> (data in Fig. 2) as well as the region flanked by P<sub>1</sub> and P<sub>2</sub> (data in Fig. 3), an initial PCR was performed with the following primers, specific for bisulfite-treated DNA: ATT CGT AAA AGT GAT TTA TCG TTG TGT T (upper primer) and ACC TCC CCA AAT CCC AAA AAC TAA AAC T (lower primer). These primers were designed to be complementary to nucleotides -1206 to -1179 and 985 to 1012, respectively of bisulfite-converted DNA (assigning P<sub>1</sub> transcription initiation site as +1). PCRs included 0.5  $\mu$ M each primer, 0.2  $\mu$ M dNTPs, 2.5 mM MgCl<sub>2</sub>, 50 mM KCl, 10 mM Tris (pH 8.3), 2  $\mu$ l of bisulfite-treated genomic DNA, and 5 units of Taq polymerase (Perkin Elmer Corp., Norwalk, CT) in a final volume of 50  $\mu$ l. Following initial denaturation at 95°C for 3 min, 38 cycles, consisting of 95°C for 1 min, 54°C for 90 sec, and 72°C for 3 min, commenced. In all PCRs, polymerase was added after the heat block had reached 95°C to effect a hot start of the amplification.

The product of the initial PCR was used as template for a second PCR, using nested primers. To amplify the genomic region upstream of P<sub>1</sub>, the following primers were used: GAG TGA GAT GGG GTG GAG CGG TAT TTA TTT (upper primer) and CGT CCG ACC CGA TCT ACT CTC CCT CCT AAT (lower primer), corresponding to nucleotides -1107 to -1078 and -343 to -314, respectively. Similarly, the region of genomic DNA flanked by P<sub>1</sub> and P<sub>2</sub> was amplified using the following nested primers: GGA AGA GGC GTG CGA GAG AAG GAA TAA T (upper primer) and CCA AAA AAC GCT AAC AAC CCT AAA AAC GAA A (lower primer), corresponding to nucleotides 136 to 163 and 906 to 936, respectively. For these nested amplifications, 1  $\mu$ l of the initial PCR reaction product was used as template, in a PCR with 0.5  $\mu$ M each primer, 0.2  $\mu$ M dNTPs, 2.5 mM MgCl<sub>2</sub>, 50 mM KCl, 10 mM Tris (pH 8.3), and 5 units of Taq polymerase in a final volume of 25  $\mu$ l. The PCR profile was the same as in the initial PCR, except that 42 cycles were performed.

A different set of initial and nested PCR primers were used to amplify the region flanking the transcription initiation site of P<sub>2</sub> and extending to the start of the first intron. Initial PCR amplification used the following primers: ATT TTA TAT TTT AGT TAA TGA AGA YGA GAG GT (upper primer) and AAC TCC CAA CTC CAA TTC AAA CCC TCC A (lower primer), where "Y" denotes a 50% C-50% T mixture. These primers corresponded to nucleotides 367 to 398 and 1489 to 1516 of the bisulfite-converted sequence, respectively. PCR conditions were as indicated above for the initial PCR, except that only 2 units of polymerase were used in a final volume of 40  $\mu$ l, and the annealing temperature was 50°C. The nested primers for this region were: TTC GAG GAA GTG TAA ATA AAA GAG AAA GTA TG (upper primer) and CAA ACC CTC CAA CAC AAA CAC CCC AAC R (lower primer), where "R" denotes a 50% G-50% A mixture. These primers corresponded to nucleotides 426 to 457 and 1472 to 1499 of the bisulfite-converted sequence, respectively. For this nested PCR, 1  $\mu$ l from the initial PCR was used as template, and the annealing temperature was 52°C for 40 cycles.

PCR products from the nested reactions were subcloned using the pGEM-T Vector System (Promega). Miniprep DNA was prepared from multiple clones for each reaction according to the procedure from Zhou *et al.* (12). From the clones containing the anticipated DNA insert, identified by restriction enzyme digests, DNA for sequencing was prepared using the Plasmid Mini Kit (Qiagen, Chatsworth, CA). DNA sequencing was performed using the ABI Prism Big Dye Terminator Cycle Sequencing System (Perkin Elmer Corp.). M13-based sequencing primers, complementary to the plasmid backbone, were used. PCR conditions consisted of denaturing for 30 s at 96°C, annealing for 15 s at 50°C, and extension for 4 min at 60°C. This cycle was repeated 25 times. Sequencing PCR solutions were purified using Centriflex Gel Filtration Cartridges (Advanced Genetic Technologies, Gaithersburg, MD), as described in the manufacturer's instructions. The known genomic DNA sequence (8, 9) was compared to the sequence derived from the bisulfite-treated DNA for each clone. In this way, the methylation status of each CpG was determined because unmethylated cytosines appeared as thymidines in the bisulfite-treated DNA, whereas methylated cytosines were shown as cytosines.

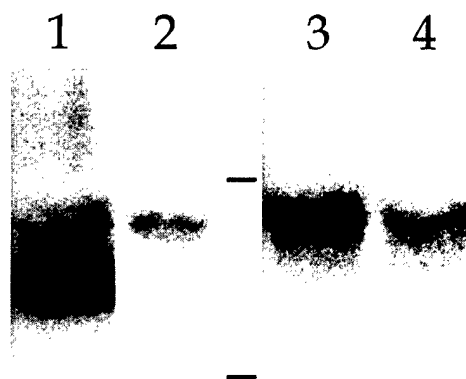


Fig. 1. Northern blot analysis of TGF- $\beta$ 3 expression. Total RNA (25  $\mu$ g) from cells grown in tissue culture was loaded in each lane. Lanes 1 (T47-D) and 2 (HT-1080) are from one experiment; Lanes 3 (HT-1080) and 4 (A375) are from a second experiment. Equivalent loading of RNA was documented by ethidium bromide staining. For the purpose of band intensity comparisons, the exposure and contrast levels of Lanes 1 and 2 are identical, as are those of Lanes 3 and 4. The positions of the 18S and 28S RNA in the gel are indicated by bars in the center of the figure.

## Results

We have previously reported that human breast cancer cell lines that express TGF- $\beta$ 3 do so by transcription from two promoters, generating two mRNA transcripts which differ in their 5' noncoding regions (10). As shown in Fig. 1, RNA from the T47-D cell line demonstrates two bands on Northern analysis when a probe from the TGF- $\beta$ 3 coding region is used. In contrast, RNA from two cell lines that transcribe TGF- $\beta$ 3 only from P<sub>1</sub> (HT1080 and A375, sarcoma and melanoma cell lines, respectively) contain only the full-length 3.5-kb transcript (Fig. 1).<sup>4</sup> Initial efforts at mapping the CpG methylation status at the TGF- $\beta$ 3 gene locus were focused on the main core of the CpG island. Genomic DNA was isolated from cells grown in culture, treated according to a modification of the bisulfite method for distinguishing between methylated and unmethylated cytosines, PCR-amplified, subcloned, and sequenced. Sequence data from multiple clones from each cell line were used to calculate cell type-specific estimates of percentage methylation at each CpG site.

Data from the HT1080 sarcoma cells are plotted in Fig. 2, along with data from two breast cancer cell lines that transcribe from both P<sub>1</sub> and P<sub>2</sub> (SKBR-3 and T47-D). Located at the top of Fig. 2, a scaled map of CpG site locations shows the high-density core region of the island in which we have mapped methylation status. Cumulative data derived from sequence information from multiple clones ( $n = 4-13$  for each CpG site, for each cell line) are plotted in the graph at the bottom of the figure. There were isolated CpGs showing >40% methylation in the upstream half of this region, whereas methylation was minimal or absent in the 3' portion of the island core. Overall, the majority of CpG sites in this region of the island were only minimally methylated, and there was no evident methylation pattern that was correlated with promoter usage.

A similar series of experiments were performed to map CpG methylation status in a region of genomic DNA flanked by the two promoters. This is a less CpG-dense region, downstream of the high density CpG core of this island complex. As is evident in Fig. 3, most of these CpG sites exhibited minimal methylation in all three cell lines, with the notable exception of the five 3'-most CpG sites. These CpGs, which flank the P<sub>2</sub> transcription initiation site, were nearly

<sup>4</sup> RNA analysis of TGF- $\beta$ 3 expression for the other cell lines used in this work can be found in Ref. 10.

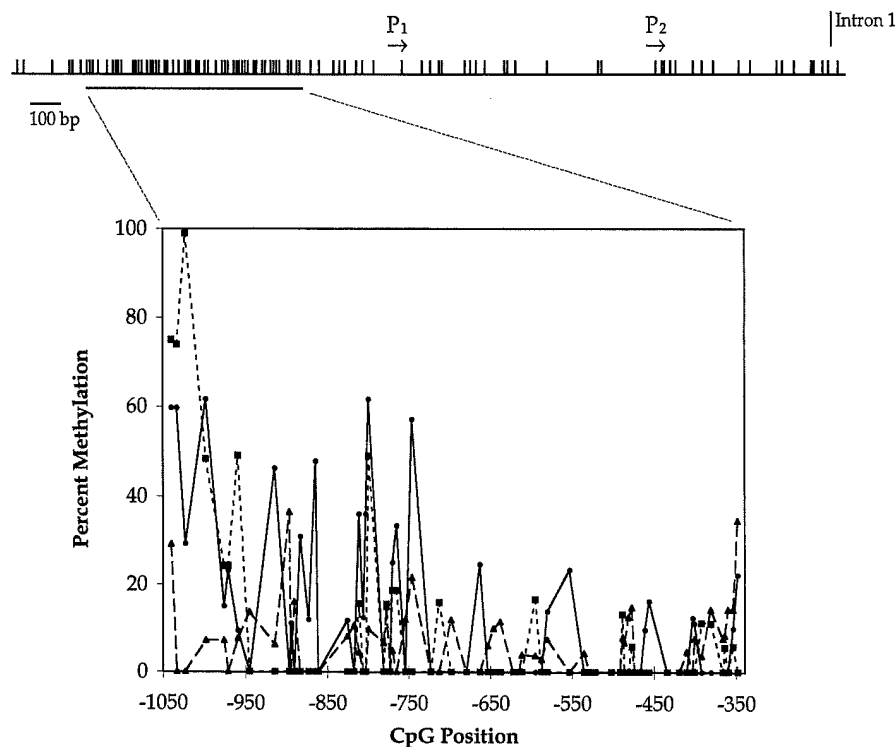


Fig. 2. Methylation within the CpG island core in the TGF- $\beta$ 3 promoter. The locations of CpGs within the genomic region encompassing TGF- $\beta$ 3's two promoters and first exon are indicated by hatch marks above the linear representation of genomic DNA, and the region within the core of the CpG island investigated by DNA sequence analysis of bisulfite-treated DNA is indicated by the line below. Graphically represented is the percentage methylation at each CpG site within this region observed in DNA from HT1080 cells (●), SKBR-3 cells (■), and T47-D cells (▲). Data points, average of multiple sequence determinations for each CpG site for each cell line ( $n = 4-20$ ).

completely methylated in the HT1080 cells, but remained unmethylated in SKBR-3 and T47-D cells.

The magnitude of the differences at these CpG sites suggested to us that high levels of methylation at selected CpG sites surrounding the downstream promoter ( $P_2$ ) may be a mechanism by which non-breast cancer cells block activation of  $P_2$  and, therefore, restrict transcription initiation of TGF- $\beta$ 3 to the upstream promoter. To explore that

possibility, we broadened our panel of cell lines to include an additional two that use TGF- $\beta$ 3's  $P_1$  only: A375 (melanoma) and A673 (lung cancer). For each of the five cell lines, we mapped the CpG methylation frequency for the region of genomic DNA extending from the CpG at position 525 to the CpG at position 1472, located in the 5' portion of the first intron. Thus, a total of 22 CpG sites were investigated in this set of experiments. As is evident in Fig. 4, the

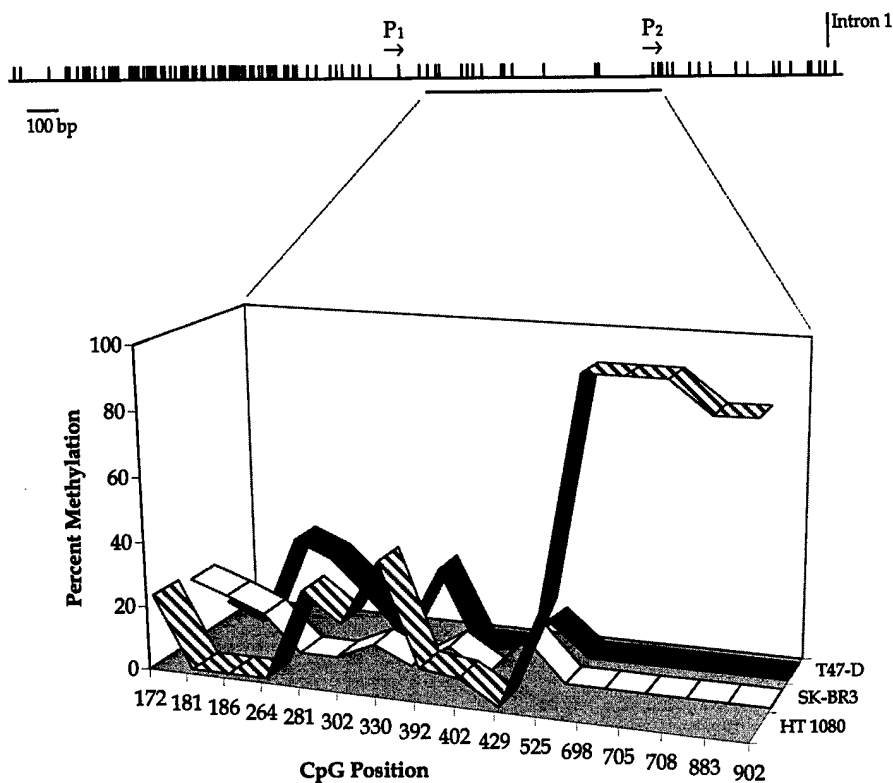


Fig. 3. Methylation at CpG sites flanked by the two transcription initiation sites for TGF- $\beta$ 3. Top, the region of genomic DNA investigated in this series of experiments is indicated by the line just beneath the CpG map, as in Fig. 1. Percentage methylation at each of the indicated CpG positions (numbered with +1 = transcription initiation site of  $P_1$ ) represents the average of multiple sequence determinations from bisulfite-treated DNA from HT1080 cells (▨), SKBR-3 cells (□), and T47-D cells (■;  $n = 4-18$ ).



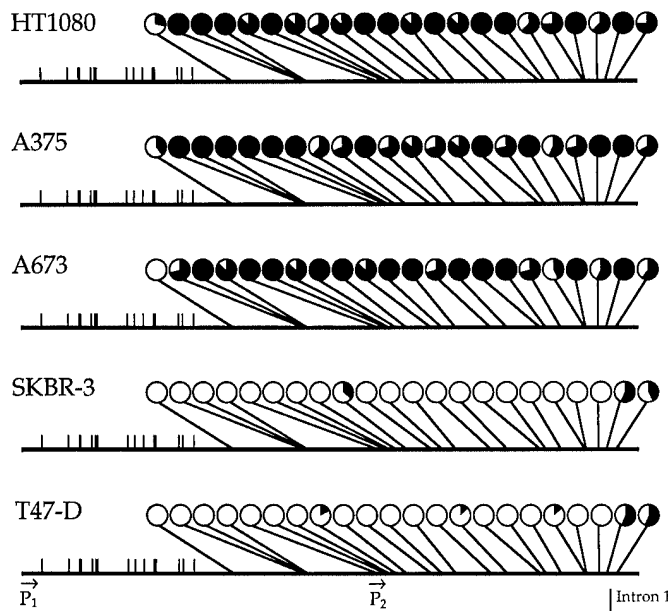


Fig. 4. Methylation at CpG sites flanking the downstream, breast cancer-specific TGF- $\beta$ 3 promoter ( $P_2$ ). The percentage methylation at the investigated CpG sites is represented by small pie graphs, with the percentage of area filled-in proportional to the frequency of methylation, as determined from sequence analysis of four to eight clones at each CpG site for each of the indicated cell lines. For example, the 3'-most investigated CpG (position 1472) exhibited a 75% incidence of methylation in HT1080 cells and a 43% incidence of methylation in SKBR-3 cells. The investigated CpG sites are located at positions 525, 698, 705, 708, 883, 902, 910, 928, 953, 1014, 1041, 1075, 1161, 1201, 1284, 1297, 1334, 1393, 1398, 1429, 1449, and 1472, relative to  $P_1$ .

incidence of methylation in this region is strikingly different when the non-breast cancer cell lines (HT1080, A375, and A673) are compared to breast cancer cell lines (SKBR-3 and T47-D). This difference is most notable for the 19 CpGs from positions 698 to 1429. Within this region, the non-breast cancer cell lines demonstrated high levels of methylation (average = 88%), whereas the breast cancer cell lines exhibited pronounced hypomethylation (average = 1%).

## Discussion

One of the well-recognized strategies for regulation of gene expression is the use of alternative promoters in a tissue-specific or developmentally specific pattern (13). In some cases, the different promoters yield mRNA transcripts that share coding regions but differ in their 5' UTRs. Although the presence of different 5' UTR sequences in mRNAs encoding the same protein potentially allows for transcript-specific regulation of mRNA localization and stability, the bulk of prior work on the influence of the 5' UTR suggests that such transcripts might primarily differ in translational capacity (14). In this manner, promoter usage could affect protein levels at the posttranscriptional level.

One example of a gene with two promoters that generate mRNA transcripts with differing translational efficiency but encode the same protein, is TGF- $\beta$ 3. Prior work in our laboratory has documented the presence of a downstream promoter, active only in breast cancer cells, that results in a 5' truncated transcript with enhanced translational capacity (10). Other examples of alternative promoters resulting in differing 5' UTRs include the insulin-like growth factor-II gene (15) and the neuronal nitric oxide synthase gene (16). An interesting feature of the TGF- $\beta$ 3 genetic locus, shared by the neuronal nitric oxide synthase gene, is that the two alternative promoters are in close proximity to each other and are associated with a CpG island.

Although methylation of CpG islands associated with the promoter regions of certain genes has been implicated as a mechanism of repressed transcription, there has been little investigation into how methylation may be involved with differential use of alternative promoters. Frequently, the methylation status of a CpG island is determined by characterization of a relatively few number of CpGs within the core of the island. Two commonly used methodologies are methylation-specific PCR, in which primers specific to methylated versus unmethylated CpGs are used to amplify bisulfite-treated DNA, and the use of methylation-sensitive restriction enzymes (4, 17, 18). Both approaches provide information regarding a small subset of CpGs within the island complex, and may therefore lack the requisite sensitivity to evaluate the role of CpG methylation in the utilization of alternative promoters.

We have, therefore, approached our examination of the TGF- $\beta$ 3

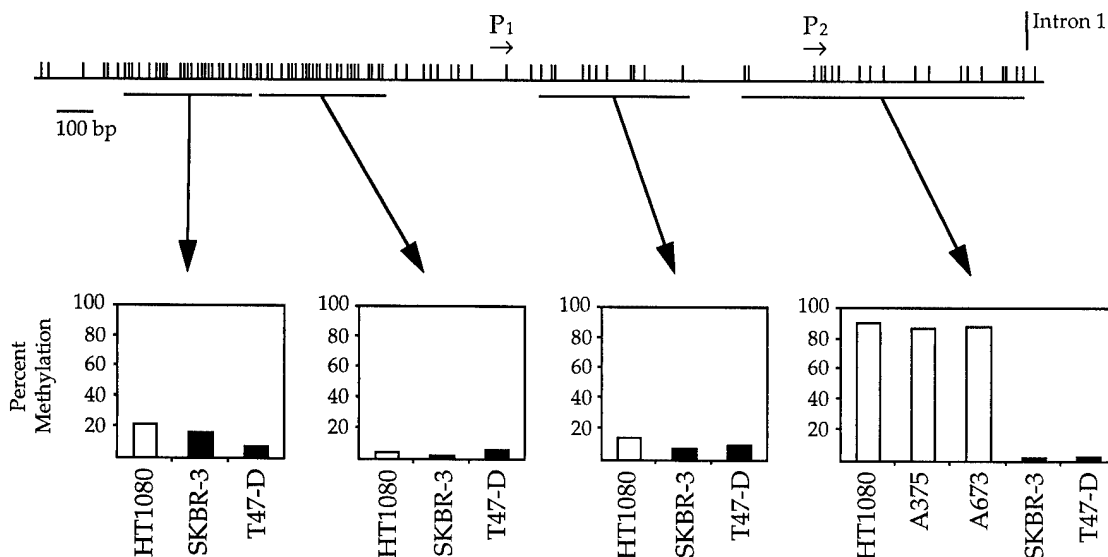


Fig. 5. Summary of cell-specific CpG methylation throughout the TGF- $\beta$ 3 CpG archipelago. The investigated CpGs were divided into four regional groupings, as indicated by the lines beneath the CpG map (top). The average incidence of methylation for all CpG sites within each region is shown for the indicated cell lines. ■, two breast cancer cell lines (SKBR-3 and T47-D); □, non-breast cancer cell lines (HT1080, A375, and A673).

locus by comprehensive sequence analysis of large regions of the associated CpG island. A composite overview of our findings, including data from multiple cell lines regarding methylation within the indicated CpGs, is presented in Fig. 5. It is clear from our data that dramatic differences in CpG methylation between breast and non-breast cancer cell lines are restricted to a relatively small subset of CpGs that flank the downstream promoter. The hypermethylation at these sites in all of the non-breast cancer cell lines is consistent with the transcriptional suppression of this promoter in these cells. These observations have suggested to us that many CpG islands, such as that associated with TGF- $\beta$ 3, should more appropriately be considered as an island chain or CpG archipelago, composed of many islands of varying density. Such a view would facilitate recognition of the potential importance of methylation that is restricted to one portion of the island chain, which in our case is evident in the 3' tail of the CpG archipelago.

In summary, we have shown that methylation within most of the CpG island of TGF- $\beta$ 3 does not differ between breast and non-breast cancer cell lines, but that the lack of cytosine methylation in the region proximal to P<sub>2</sub> may underlie its transcription activation in breast cancer cells, thereby yielding a mRNA with enhanced translational capacity.

## References

1. Comb, M., and Goodman, H. M. CpG methylation inhibits proenkephalin gene expression and binding of the transcription factor AP-2. *Nucleic Acids Res.*, **18**: 3975-3982, 1990.
2. Tate, P. H., and Bird, A. P. Effects of DNA methylation on DNA-binding proteins and gene expression. *Curr. Opin. Genet. Dev.*, **3**: 226-231, 1993.
3. Lapidus, R. G., Nass, S. J., Butash, K. A., Parl, F. F., Weitzman, S. A., Graff, J. G., Herman, J. G., and Davidson, N. E. Mapping of ER gene CpG island methylation by methylation-specific polymerase chain reaction. *Cancer Res.*, **58**: 2515-2519, 1998.
4. Lapidus, R. G., Ferguson, A. T., Ottaviano, Y. L., Parl, F. F., Smith, H. S., Weitzman, S. A., Baylin, S. B., Issa, P. J., and Davidson, N. E. Methylation of estrogen and progesterone receptor gene 5' CpG islands correlates with lack of estrogen and progesterone receptor gene expression in breast tumors. *Clin. Cancer Res.*, **2**: 805-810, 1996.
5. Ohtani-Fujita, N., Fujita, T., Aoike, A., Osifchin, N. E., Robbins, P. D., and Sakai, T. CpG methylation inactivates the promoter activity of the human retinoblastoma tumor-suppressor gene. *Oncogene*, **8**: 1063-1067, 1993.
6. Graff, J. R., Herman, J. G., Lapidus, R. G., Chopra, H., Xu, R., Jarrard, D. F., Isaacs, W. B., Pitha, P. M., Davidson, N. E., and Baylin, S. B. E-cadherin expression is silenced by DNA hypermethylation in human breast and prostate carcinomas. *Cancer Res.*, **55**: 5195-5199, 1995.
7. Mancini, D. N., Rodenhiser, D. I., Ainsworth, P. J., O'Malley, F. P., Singh, S. M., Xing, W., and Archer, T. K. CpG methylation within the 5' regulatory region of the *BRCA1* gene is tumor specific and includes a putative CREB binding site. *Oncogene*, **16**: 1161-1169, 1998.
8. Lafyatis, R., Lechleider, R., Kim, S.-J., Jakowlew, S., Roberts, A. B., and Sporn, M. B. Structural and functional characterization of the transforming growth factor  $\beta$ 3 promoter. A cAMP-responsive element regulates basal and induced transcription. *J. Biol. Chem.*, **265**: 19128-19136, 1990.
9. Arrick, B. A., Lee, A. L., Grendell, R. L., and Derynck, R. Inhibition of translation of transforming growth factor- $\beta$ 3 mRNA by its 5' untranslated region. *Mol. Cell. Biol.*, **11**: 4306-4313, 1991.
10. Arrick, B. A., Grendell, R. L., and Griffin, L. A. Enhanced translational efficiency of a novel transforming growth factor- $\beta$ 3 mRNA in human breast cancer cells. *Mol. Cell. Biol.*, **14**: 619-628, 1994.
11. Raizis, A. M., Schmitt, F., and Jost, J.-P. A bisulfite method of 5-methylcytosine mapping that minimizes template degradation. *Anal. Biochem.*, **226**: 161-166, 1995.
12. Zhou, C., Yang, Y., and Jong, A. Y. Mini-prep in ten minutes. *BioTechniques*, **8**: 172-173, 1990.
13. Ayoubi, T. A. Y., and Van de Ven, W. J. M. Regulation of gene expression by alternative promoters. *FASEB J.*, **10**: 453-460, 1996.
14. Kozak, M. An analysis of vertebrate mRNA sequences: intimations of translational control. *J. Cell Biol.*, **115**: 887-903, 1991.
15. Nielsen, F. C., Gammeltoft, S., and Christiansen, J. Translational discrimination of mRNAs coding for human insulin-like growth factor II. *J. Biol. Chem.*, **265**: 13431-13434, 1990.
16. Xie, J., Roddy, P., Rife, T. K., Murad, F., and Young, A. P. Two closely linked but separable promoters for human neuronal nitric oxide synthase gene transcription. *Proc. Natl. Acad. Sci. USA*, **92**: 1242-1246, 1995.
17. Herman, J. G., Graff, J. R., Myöhänen, S., Nelkin, B. D., and Baylin, S. B. Methylation-specific PCR: a novel PCR assay for methylation status of CpG islands. *Proc. Natl. Acad. Sci. USA*, **93**: 9821-9826, 1996.
18. Xiong, Z., and Laird, P. W. COBRA: a sensitive and quantitative DNA methylation assay. *Nucleic Acids Res.*, **25**: 2532-2534, 1997.